Evolution of the electronic properties of Sn_n^- clusters ($n=4-45$) and the semiconductor-to-metal transition

Li-Feng Cui, Lei-Ming Wang, and Lai-Sheng Wang[a)]
Department of Physics, Washington State University, Richland, Washington 99354 and Chemical Sciences Division, Pacific Northwest National Laboratory, MS K8-88, P.O. Box 999, Richland, Washington 99352

(Received 23 October 2006; accepted 28 December 2006; published online 13 February 2007)

The electronic structure of Sn_n^- clusters ($n=4-45$) was examined using photoelectron spectroscopy at photon energies of 6.424 eV (193 nm) and 4.661 eV (266 nm) to probe the semiconductor-to-metal transition. Well resolved photoelectron spectra were obtained for small Sn_n^- clusters ($n\leqslant 25$), whereas more congested spectra were observed with increasing cluster size. A distinct energy gap was observed in the photoelectron spectra of Sn_n^- clusters with $n\leqslant 41$, suggesting the semiconductor nature of small neutral tin clusters. For Sn_n^- clusters with $n\geqslant 42$, the photoelectron spectra became continuous and no well-defined energy gap was observed, indicating the onset of metallic behavior for the large Sn_n clusters. The photoelectron spectra thus revealed a distinct semiconductor-to-metal transition for Sn_n clusters at $n=42$. The spectra of small Sn_n^- clusters ($n\leqslant 13$) were also compared with those of the corresponding Si_n^- and Ge_n^- clusters, and similarities were found between the spectra of Sn_n^- and those of Ge_n^- in this size range, except for Sn_{12}^-, which led to the discovery of stannaspherene (the icosahedral Sn_{12}^{2-}) previously [L. F. Cui *et al.*, J. Am. Chem. Soc. **128**, 8391 (2006)]. © *2007 American Institute of Physics*. [DOI: 10.1063/1.2435347]

I. INTRODUCTION

Atomic clusters of the group 14 elements have been the topic of intensive studies in cluster science because of their major scientific and technological importance. One of the key questions concerns the growth pattern and bonding behavior of these clusters as a function of size. The trend going down the periodic table is fascinating for the group 14 elements, from the semimetallic graphite (or wide band gap diamond) to the semiconductors Si and Ge to the metallic Sn and Pb. Carbon clusters have been found to undergo interesting structural variations with the increase of cluster size from linear chains to monocyclic rings to polycyclic rings to fullerenes and carbon nanotubes. Small Si and Ge clusters seem to exhibit tetrahedral bonding feature found in the bulk semiconductors.[1–28] Ion mobility experiments have revealed that they form prolate structures in the smaller size regime and undergo a structural transition to more spherical geometries at the size of several dozen atoms.[16–20] Relative to its lighter congeners, clusters of tin have attracted less attention. The growth behavior of tin clusters has been suggested in general to resemble those of Ge and Si clusters on the basis of ion mobility data.[29,30] Interestingly, the melting temperatures of tin clusters have been reported to be abnormally high relative to that of the bulk.[31] This finding has drawn significant recent attention to tin clusters,[32–38] although the nature of the abnormal melting temperature has not been fully elucidated. It is clear that knowledge of the electronic and atomic structures and the nature of the chemical bonding in these clusters would be essential for a proper understanding of their melting behavior or other physical and chemical properties.

Bulk tin possesses two allotropes. Besides the metallic form (β-Sn) under ambient conditions, there also exists a semiconducting form (α-Sn) below 286 K.[39] Crystalline α-Sn has the same tetrahedral diamond lattice as Si and Ge with a very small band gap. Therefore, the nature of the chemical bonding in tin clusters is of great interest. Are tin clusters metallic- or semiconductorlike? How do they evolve as a function of size?

The mass spectra of tin clusters produced by various techniques have been compared with those of Si_n, Ge_n, and Pb_n by several groups.[40–42] But the arguments regarding the resemblance between the mass abundance spectra of Sn_n and those of Si_n, Ge_n, and Pb_n have not been very informative, because it is well known that mass abundances are strongly dependent on source conditions or methods of production. The size dependence of ionization potentials has been shown to be similar between Sn_n and Si_n/Ge_n clusters for $n\leqslant 12$, but it displays different behavior in the medium size range of $n=15-41$.[43] Studies of Shvartsburg and Jarrold[29,30] suggested that tin clusters, similar to silicon and germanium clusters, gradually rearrange from prolate to near spherical structures at the size range of $n=35-65$, passing through several intermediate structural transitions.

A number of theoretical studies have also been carried out to investigate the electronic and atomic structures of small neutral and anion tin clusters.[32–36,44–48] Prior studies all predicted the lowest energy structures for neutral Sn_n clusters with $n\leqslant 7$ to be identical to those for Si_n and Ge_n clusters. Lu *et al.*[48] found that for $n\leqslant 7$, and $n=10$ and 12, Si_n, Ge_n,

[a)]Electronic mail: ls.wang@pnl.gov

and Sn_n clusters share similar structures, whereas Sn_8 and Sn_9 have different structures compared with those of the corresponding Si and Ge clusters. A more extensive study of the low lying isomers of neutral Sn_n clusters up to $n=20$ has been carried out by Majumder *et al.*,[32,33] who suggested deviations from the growth behavior of Si and Ge clusters in the size range of $n \geqslant 8$.

Photoelectron spectroscopy (PES) of size-selected anion clusters is a powerful technique to probe the electronic structures of atomic clusters. PES studies of tin clusters have been performed by several groups previously.[49–51] The prior PES results[50,51] suggest that the photoelectron spectra of Sn_n^- clusters are similar to those of Sn_n^- and Ge_n^- consistent with the ion mobility studies concerning the structural similarity between Sn and Si/Ge clusters. In particular, Negishi *et al.*[51] reported an extensive set of PES data on Sn_n^- clusters and used halogen doping to probe the nature of the electronic structure in Sn_n and Pb_n clusters. Their PES data suggested that a small band gap exists in small Sn_n clusters. But the semiconductor-to-metal transition was not conclusively observed due to the limited size range and/or spectral resolution.

All the previous PES works on Sn_n^- clusters have been done with photon energies at 4.661 eV (266 nm) or less and at relatively poor spectral resolution. We are interested in probing the electronic structure evolution of Sn_n^- clusters, in particular, the semiconductor-to-metal transition, at higher photon energies and improved spectral resolution. High photon energies allow more valence transitions to be observed, whereas the improved spectral resolution would allow more definitive observation of the energy gap. Our improved data immediately revealed that the spectra of Sn_{12}^- are unusual relative to those of its neighbors and are totally different from those of Si_{12}^- and Ge_{12}^-. That led to the recent discovery of stannaspherene (Sn_{12}^{2-}) (Ref. 38) and subsequently plumbaspherene (Pb_{12}^{2-}),[52] which are highly stable icosahedral cages with large empty interiors analogous to the fullerene C_{60}. The chemical bonding in stannaspherene and plumbaspherene is similar to the well-known $B_{12}H_{12}^{2-}$ molecule. The stannaspherene and plumbaspherene cages have diameters larger than 6 Å and can host all transition metal atoms to form a class of stable endohedral cage clusters,[53] even more advantageous than endohedral fullerenes, which cannot entrap transition metal atoms other than the rare earth elements.[54]

In the current work, we report the details of our PES study on Sn_n^- ($n=4-45$) at 193 nm (6.424 eV) and 266 nm (4.661 eV) under well controlled experimental conditions and with improved spectral resolution. The new data allow us to obtain more accurate electron affinities (EAs), as well as better defined spectral features. The energy gap is also better determined, showing a clear closing at $n=42$, which defines the cluster size of semiconductor-to-metal transition. The trend of the EAs as a function of size also indicates that for $n>41$ it follows the metallic droplet model, consistent with the nonmetal to metal transition at $n=42$.

II. EXPERIMENTAL METHODS

The experiment was carried out using a magnetic-bottle time-of-flight photoelectron spectrometer, details of which have been described elsewhere.[55] The Sn_n^- cluster anions were produced by laser vaporization of a pure tin target with a helium carrier gas and analyzed using a time-of-flight mass spectrometer. The Sn_n^- ($n=4-45$) clusters were each mass selected and decelerated before crossing with a detachment laser beam in the interaction zone of the magnetic-bottle photoelectron analyzer. In the current study, two detachment photon energies were used, 266 nm Nd:YAG (4.661 eV) from a (neodynium doped yttrium aluminum garnet) laser and 193 nm (6.424 eV) from an ArF excimer laser. Well resolved photoelectron spectra were obtained by carefully selecting those clusters that had sufficient resident time in the nozzle to be thermalized. We have shown previously that clusters with long resident time in the nozzle are relatively cold, which are essential to yield well resolved PES spectra.[56,57] Photoelectrons were collected at nearly 100% efficiency by the magnetic bottle and analyzed in a 3.5-m-long electron flight tube. The binding energy spectra were obtained by subtracting the kinetic energy spectra from the photon energies of the detachment laser. The spectra were calibrated using the known spectrum of Au^- for the 193 nm spectra and Pt^- for the 266 nm data. The apparatus had an electron energy resolution of $\Delta E/E \approx 2.5\%$, i.e., about 25 meV for 1 eV electrons. We also obtained photoelectron spectra for Si_n^- and Ge_n^- clusters in the smaller size regime under similar experimental conditions for comparison with the Sn_n^- clusters.

III. EXPERIMENTAL RESULTS

A. The 193 nm spectra of Sn_n^- ($n=4-45$)

The 193 nm spectra of Sn_n^- are shown in Fig. 1 for ($n=4-45$). For $n<10$, spectral features appeared only below 5 eV, but for larger clusters high binding energy features were observed, which could only be accessed at 193 nm. All spectra were well resolved for $n \leqslant 25$ and the PES spectra in this size range showed strong size dependence, where adding or removing one Sn atom produced major changes to the PES spectrum. Relatively simple spectra with well resolved features were observed for clusters with $n<10$. For $n \geqslant 10$, the spectral features became more congested, except for Sn_{12}^-, which exhibited a relatively simple spectrum with only five resolved features. It was this observation that led to our discovery of stannaspherene previously.[38]

A clear energy gap was observed in most of the PES spectra, where a relatively weak threshold band was followed by an energy gap and more intense transitions at higher binding energies. This observation suggests that the neutral Sn clusters are closed shell and the extra electron in the anion occupies the lowest unoccupied molecular orbital (LUMO) of the neutral system, giving rise to the relatively weak threshold feature. Sn_4^- and Sn_7^- exhibited the largest energy gaps of 0.93 and 1.25 eV, respectively, suggesting that neutral Sn_4 and Sn_7 are highly stable clusters. A number of clusters were observed to have relatively small gaps, including $n=5$, 8, 10, and 12 in the size range below $n=25$.

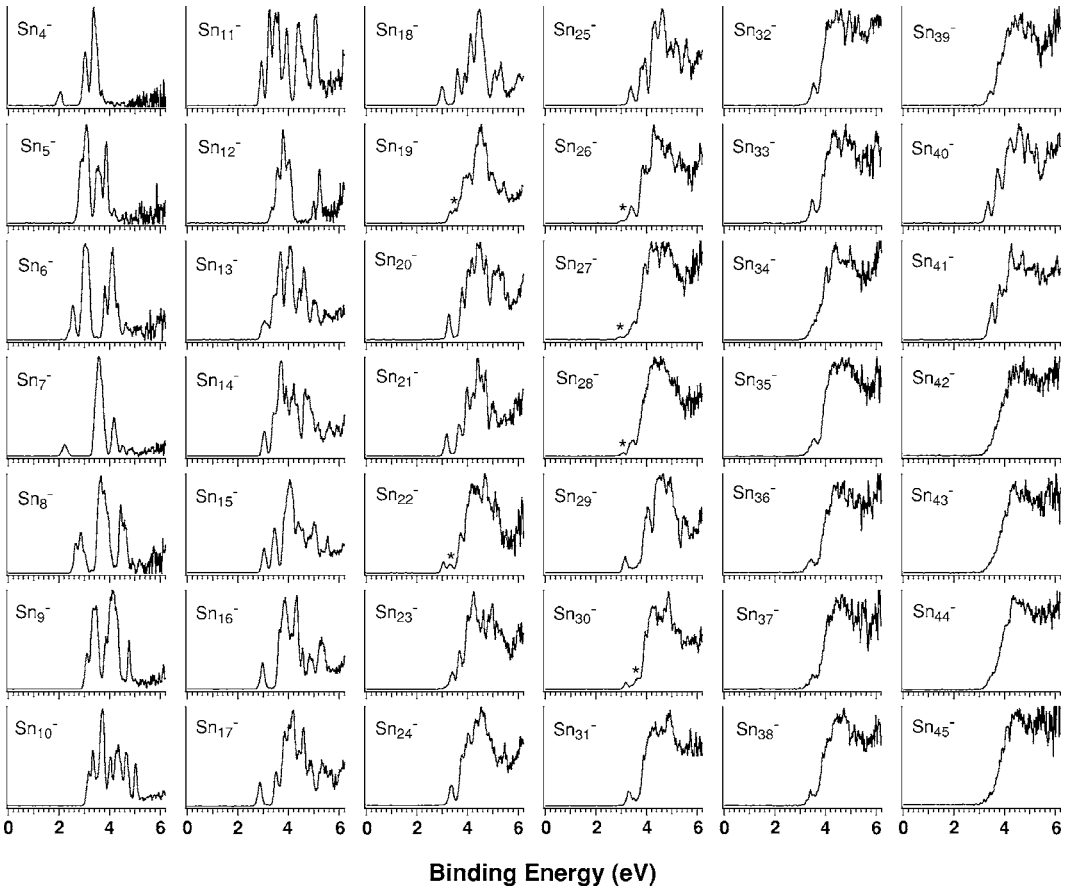

FIG. 1. Photoelectron spectra of Sn_n^- (n=4–45) at 193 nm (6.424 eV). "*" denotes contributions from a secondary isomer.

For Sn_{19}^- and Sn_{22}^-, a weak feature (labeled as * in Fig. 1) seemed to be observed in the band gap range, which suggested the existence of potential isomers.

For the cluster size range of $n \geqslant 26$, the PES spectra were relatively poorly resolved due to the congested electronic transitions and/or the existence of isomers. The threshold transition and a small band gap could still be resolved for all the species up to n=41, beyond which no spectral features could be resolved and the PES spectra became essentially continuous abruptly for n=42–45. The spectrum of Sn_{29}^- was relatively well resolved and showed the largest band gap of 0.73 eV in this size range, indicating that neutral Sn_{29} should be an electronically stable cluster. Weak spectral features near the threshold (labeled * in Fig. 1), which could be due to minor structural isomers, were observed in the spectra of Sn_{26}^-, Sn_{27}^-, Sn_{28}^-, and Sn_{30}^-. The threshold feature in Sn_{34}^- was not well resolved, possibly also due to the presence of isomers. However, the spectra of Sn_{40}^- and Sn_{41}^- were surprisingly well resolved compared to other species in this size range.

B. The 266 nm spectra of Sn_n^- (n=4–31)

Figure 2 shows the 266 nm spectra of Sn_n^- for n=4–31. The PES spectra of small Sn_n^- clusters (n=1–12) at 266 nm have been reported previously by Moravec *et al.*[50] Negishi *et al.*[51] have reported the 266 nm PES spectra of Sn_n^- for (n=4–45). Generally, the current PES spectra are consistent with the previous results, but significantly improved. The spectral resolution of the current study is comparable to that of Moravec *et al.*, but the signal to noise ratios were much improved, in particular, in the higher binding energy side. In all the spectra of Negishi *et al.*, a low energy tail was present likely due to hotter clusters and poor resolution, which led to much lower adiabatic detachment energies (ADEs). For example, the well resolved threshold feature in the current spectra for Sn_{12}^- yielded an ADE of 3.23±0.05 eV,[38] which also defines a relatively accurate EA for neutral Sn_{12}. This is in contrast to the 3.0–3.6 eV range reported by Moravec *et al.* and the much smaller value of 2.35±0.15 eV reported by Negishi *et al.* (see Table I).

The 266 nm spectra of Sn_n^- clusters were only taken up to Sn_{31}^- in the current study because of weak photoelectron signals for large Sn_n^- clusters, which led to significant deterioration of spectral qualities, as can be seen in Fig. 2 for n =30 and 31 already. Compared with the 193 nm spectra, the data at 266 nm were better resolved for the low binding energy features accessible at this photon energy. The first band of Sn_{13}^- at 193 nm was resolved into two peaks in the 266 nm spectrum, where the second weaker peak (labeled * in Fig. 2) might be due to an isomer. A weak feature was also observed in the highest occupied molecular orbital (HOMO)-LUMO gap region in the 266 nm spectrum of Sn_{17}^-, which was not resolved in the 193 nm spectrum and could also be due to a minor isomer. It is also worth pointing out that even though the spectrum of Sn_{12}^- was better resolved at 266 nm (Fig. 2), the uniqueness of this spectrum in comparison with

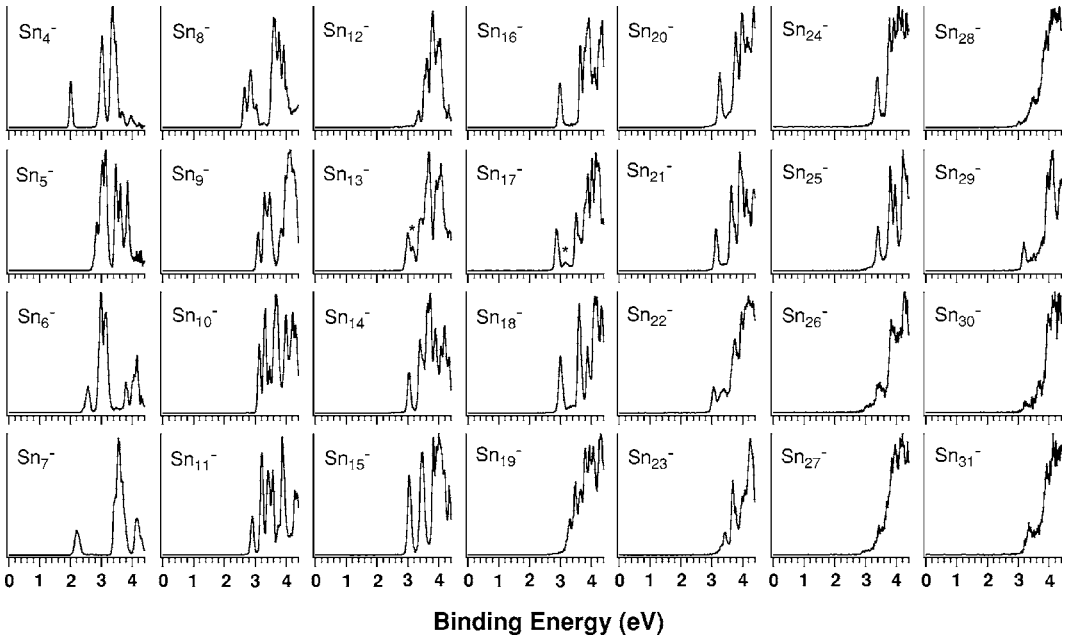

FIG. 2. Photoelectron spectra of Sn_n^- (n=4–31) at 266 nm (4.661 eV). "*" denotes contributions from a secondary isomer.

that of its neighbors was not quite obvious because of the limited spectral range, suggesting the importance of obtaining PES spectra at high photon energies or in general at various photon energies.

C. Adiabatic detachment energies and HOMO-LUMO gaps

The adiabatic detachment energies, which also represent the electron affinities of the corresponding neutral clusters, were difficult to measure in general without vibrationally resolved PES spectra. We estimated the EAs by drawing a straight line at the leading edge of the ground state feature and then adding the appropriate instrumental resolution to the intersections with the binding energy axis. Although this is an approximate procedure, we have been able to obtain consistent EAs from well resolved spectra taken at different photon energies, in particular, for spectra with a sharp onset. The relatively cold clusters in the current study resulted in

TABLE I. Electron affinities and HOMO-LUMO gaps of Sn_n clusters. All energies are in eV. (Numbers in parentheses represent the uncertainty in the last digits.)

	Electron affinity					Electron affinity		
n	Current results	Ref. 51	Ref. 50	Gaps	n	Current results	Ref. 15	Gaps
4	2.00(7)	1.79(11)	2.04(1)	0.93(7)	25	3.32(6)	2.98(12)	0.43(6)
5	2.69(6)	2.51(32)	2.65(1)	0.17(6)	26	3.31(8)	2.86(12)	0.41(8)
6	2.43(6)	2.07(13)	2.28(1)	0.43(6)	27	3.30(10)	2.80(8)	0.41(10)
7	2.10(7)	1.87(7)	1.95(10)	1.25(7)	28	3.26(8)	2.92(15)	0.36(8)
8	2.57(6)	2.39(32)	2.48(10)	0.16(6)	29	3.11(4)	2.92(7)	0.73(4)
9	3.01(5)	2.74(5)	2.5–3.1	0.22(5)	30	3.11(8)	3.00(8)	0.63(8)
10	3.06(5)	2.76(11)	3.0–3.15	0.16(5)	31	3.19(8)	2.97(11)	0.52(8)
11	2.83(5)	2.47(5)	2.7–2.95	0.32(5)	32	3.38(8)	2.98(15)	0.33(8)
12	3.23(6)[a]	2.35(15)	3.0–3.6	0.25(6)	33	3.36(8)	2.92(13)	0.45(8)
13	2.89(5)	2.63(9)		0.40(5)	34	3.3(1)	2.96(18)	0.52(10)
14	2.96(5)	2.68(12)		0.34(5)	35	3.3(1)	2.85(9)	0.53(10)
15	2.97(5)	2.66(4)		0.38(5)	36	3.2(1)	2.88(11)	0.57(10)
16	2.92(5)	2.62(10)		0.67(5)	37	3.3(1)	2.90(13)	0.39(10)
17	2.82(5)	2.58(4)		0.64(5)	38	3.32(8)	2.96(10)	0.41(8)
18	2.93(5)	2.68(12)		0.61(5)	39	3.30(8)	2.97(12)	0.34(8)
19	3.18(6)	2.80(18)		0.35(6)	40	3.24(8)	3.04(8)	0.41(8)
20	3.19(5)	2.82(16)		0.48(5)	41	3.37(8)	3.04(7)	0.34(8)
21	3.08(5)	2.81(9)		0.49(5)	42	3.4(1)	2.93(6)	0
22	2.98(5)	2.72(13)		0.57(5)	43	3.4(1)	2.98(12)	0
23	3.33(7)	2.94(14)		0.28(7)	44	3.4(1)	2.97(18)	0
24	3.28(6)	3.04(12)		0.45(6)	45	3.4(1)	3.01(9)	0

[a]From Ref. 38.

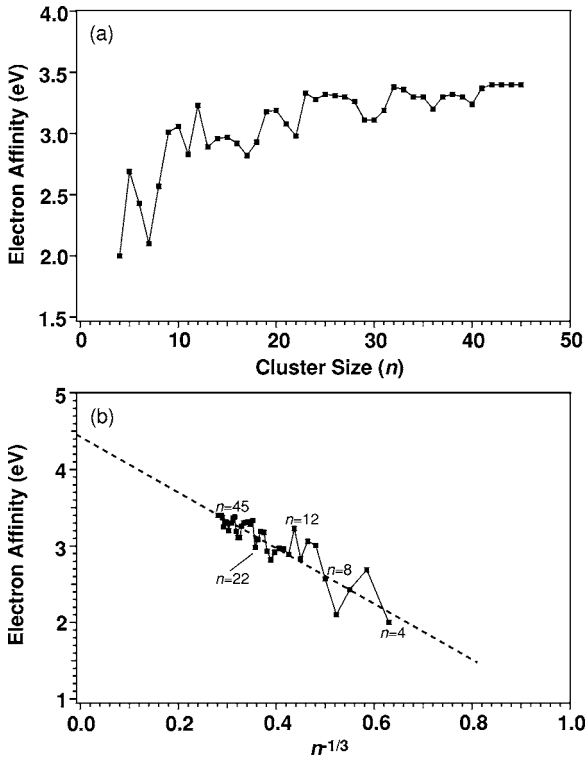

FIG. 3. (a) Electron affinities (EAs) of Sn_n (n=4–45) as a function of size n. (b) EA vs $n^{-1/3}$ ($n^{-1/3}$ is proportional to $1/r$, r being the cluster radius).

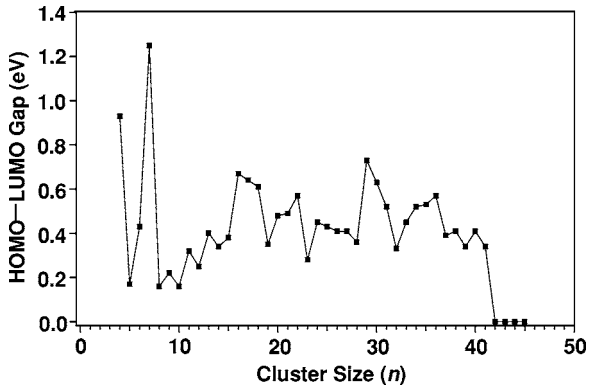

FIG. 4. HOMO-LUMO gaps of Sn_n (n=4–45) clusters as a function of size n.

better resolved spectra with sharp onsets, which were important in obtaining accurate EAs. All the reported EAs were determined from the 266 nm spectra wherever available. More accurate EAs were obtained in the lower photon energy spectra because of the better spectral resolution. The obtained EAs are compared with previous measurements in Table I and plotted as a function of size (n) and $n^{-1/3}$ in Fig. 3.

If a neutral cluster is closed shell, then in the anion the extra electron occupies the LUMO of the corresponding neutral cluster. This extra electron usually yields a weak threshold PES band followed by an energy gap, which represents the experimental measure of the HOMO-LUMO gap in the neutral cluster. This energy gap carries important information about the nonmetal to metal transition in the tin clusters. It was measured from the binding energy difference between the ADEs of the first and second PES bands. In cases where the two bands were not well resolved, we estimated the energy gaps using the peak maxima, i.e., vertical detachment energies (VDEs). The obtained values for the HOMO-LUMO gap are also given in Table I and plotted in Fig. 4.

IV. DISCUSSION

A. Sn_4^-–Sn_{10}^- and comparisons to Si_n^- and Ge_n^- clusters

In Fig. 5, we compare the PES spectra of Sn_n^- for n =4–13 to those of Si_n^- and Ge_n^- in the same size range. PES of Si_n^- and Ge_n^- has been studied extensively previously.[6–15] The current data are slightly better resolved, but otherwise consistent with the previous reports. Clearly, the spectra of the three cluster systems exhibit remarkable similarities for n=4–7, suggesting that Si, Ge, and Sn clusters possess similar structures in this size range. A number of theoretical calculations have been reported for the structures of small neutral and anion tin clusters.[32–36,44–48] The consensus is that the global minima of neutral Sn_n clusters for $n \leqslant 7$ are indeed identical to those previously established for Si_n and Ge_n species by PES and IR/Raman spectroscopy in matrices.[3,5] The relatively large energy gaps observed for n=4 and 7 (Fig. 4) are consistent with their high structural symmetries, a D_{2h} rhombus for n=4 and a D_{5h} pentagonal bipyramid for n=7. The structures for n=5 and 6 have been determined to be trigonal and tetragonal bipyramids, respectively.[32,33,46–48]

The spectra of Sn_8^-–Sn_{10}^- are similar to those of the corresponding Ge_n^- clusters, but quite different from those of the Si_n^- clusters (Fig. 5), suggesting that Sn cluster anions in this size range have similar structures to those of Ge_n^- clusters, but different from those of Si_n^-. Indeed, Sn_8 has been predicted to be a capped pentagonal bipyramid,[32] whereas Si_8 is predicted to be a distorted bicapped octahedron (C_{2h}) and Si_8^- has been confirmed to be a distorted cube (C_{2v}/C_{3v}).[20] Our PES spectral pattern for Sn_8^- displays some similarity to that of Sn_7^- (Fig. 5), providing indirect support for a capped pentagonal bipyramidal structure for Sn_8^-. Sn_9 has been predicted to be a tetracapped trigonal bipyramid,[32] which is also very different from the confirmed tricapped prism structure for Si_9^-.[12,20] For Sn_{10}, two structures with very close energies have been predicted,[32] the lowest energy structure (10a) is a distorted tetracapped prism, similar to that of Si_{10} and Si_{10}^-,[20] whereas another isomer (10b) with near C_{3v} symmetry is predicted to be only 0.09 eV higher in energy.[32] The tetracapped prism structure for Si_{10} gives the large HOMO-LUMO and has been confirmed to be the ground state also for Si_{10}^-.[12] Thus, the very different PES spectra for Sn_{10}^- can easily rule out the (10a) structure for Sn_{10}, suggesting that the near C_{3v} (10b) isomer is likely to be the ground state for Sn_{10}^-.

B. Sn_{11}^-–Sn_{13}^-: The unique PES spectra of Sn_{12}^- and the discovery of stannaspherene

In a recent communication,[38] PES spectra of Sn_n^- (n=11–13) at 193 nm have been reported and compared to those of Ge_n^- (n=11–13). In Fig. 5, we compare the spectra of Si_n^-, Ge_n^-, and Sn_n^- in the same size range. The similarities among the spectra for the 11-mer and 13-mer are obvious,

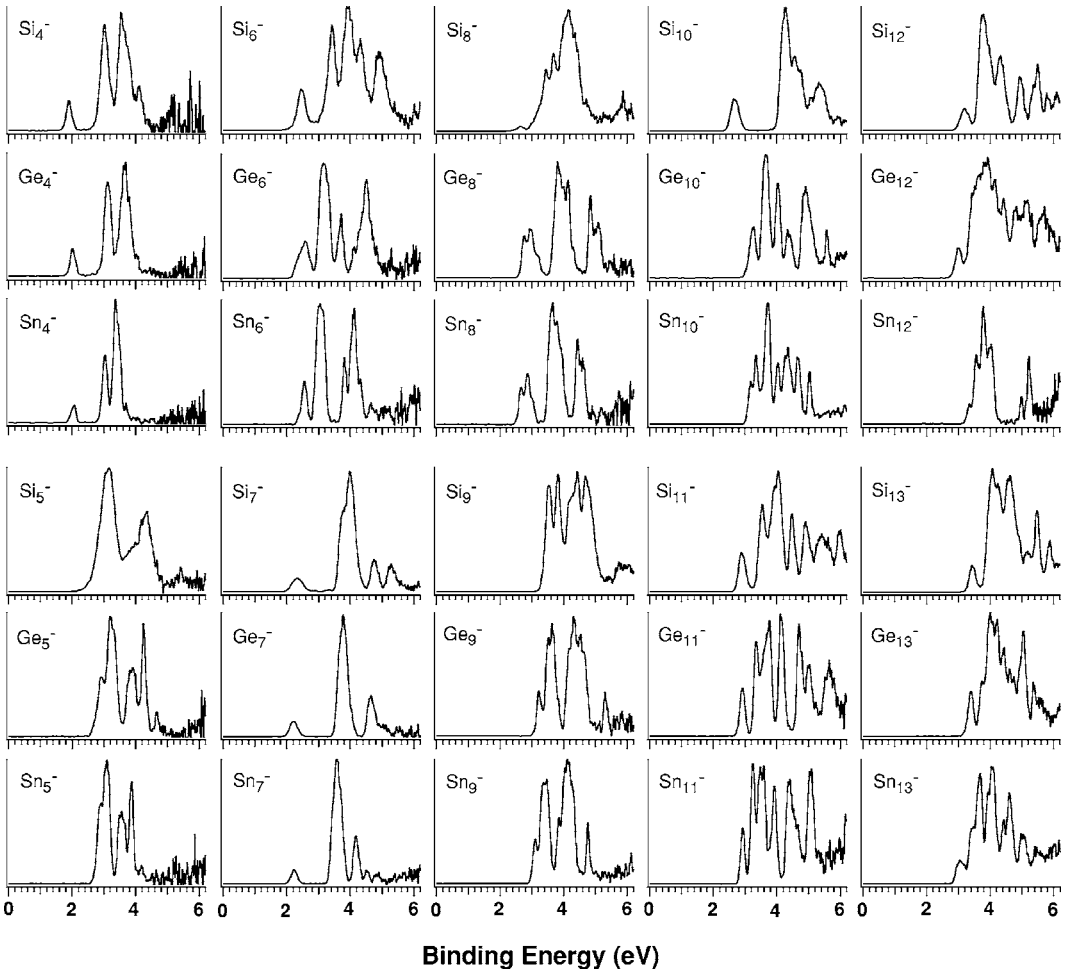

FIG. 5. Photoelectron spectra of Sn_n^- ($n=4-13$) at 193 nm compared to those of Si_n^- and Ge_n^-

suggesting that these clusters should all have similar ground state structures. The previous theoretical calculations predicting different structures for Sn_{11} and Sn_{13} from the corresponding Si_n clusters are questionable.[32] Both Si_{11}^- and Si_{13}^- have been confirmed to possess low symmetry C_s structures.[12,20] However, the PES spectrum of Sn_{12}^- is totally different from those of Sn_{12}^- and Ge_{12}^- and is also surprisingly simple compared to those of its neighbors, Sn_{11}^- and Sn_{13}^-. The relatively simple and characteristic spectrum of Sn_{12}^- immediately suggested that it should possess a high-symmetry structure, which led to our recent discovery of stannaspherene.[38] Our prior theoretical calculations showed that Sn_{12}^- is a slightly distorted icosahedral cage due to the Jahn-Teller effect. Adding an electron to Sn_{12}^- led to a perfect icosahedral cage Sn_{12}^{2-}, which possesses a large empty interior (6.1 Å diameter) and spherical π bonding similar to C_{60} and was named "stannaspherene" for its near spherical symmetry and π bonding character.[38] The stannaspherene cage is highly stable and it has been shown to be able to trap all transition metal atoms, as well as rare earth atoms, to form a whole new class of stable endohedral clusters.[53]

C. $Sn_{14}^- - Sn_{25}^-$

The PES spectra of Sn_n^- in the size range of $n=14-25$ became increasingly complicated, but were still well resolved at both 193 and 266 nm (Figs. 1 and 2). Ion mobility measurements[29,30] have suggested that tin clusters of medium size ($13 \leqslant n \leqslant 35$) adopt prolate geometries, which are similar to those found for Si_n and Ge_n.[16–28] Theoretical calculations on Sn_n ($n \leqslant 20$) (Refs. 32) showed that the structures of small tin clusters in the size range of $n=14-20$ are similar to those of Si and Ge clusters, all exhibiting prolate shapes. The PES spectra of Sn_n^- in the size range of $n=14-25$ display some similarity to those of Si_n^-,[6–11] providing additional support for their structural similarities.

In this size range, the PES spectra for several clusters, namely, Sn_{13}^-, Sn_{17}^-, Sn_{19}^-, and Sn_{22}^-, showed evidence of possible isomeric contributions. In the 266 nm spectrum of Sn_{13}^- (Fig. 2), the second weak peak around 3.2 eV (labeled "*"), which was not resolved in the 193 nm spectrum, was likely due to an isomer. Similarly, a weak feature (*) was also resolved in the energy gap region in the 266 nm spectrum of Sn_{17}^- (Fig. 2) and in both the 193 and 266 nm spectra of Sn_{19}^- and Sn_{22}^-. For Sn_{19}^- and Sn_{22}^-, this feature was fairly intense and in the 266 nm spectrum of Sn_{19}^- the second feature was even more intense than the first feature, suggesting the existence of two nearly degenerate isomers. The current data on the Sn_n^- clusters in the size range of $n=14-25$ are sufficiently well reserved and can be used to compare with more detailed theoretical calculations to elucidate the structures of tin clusters in the medium size range.

D. $Sn_{26}^- - Sn_{45}^-$

For Sn_n^- clusters with $n>25$, the PES spectra became more congested and poorly resolved. In a number of cases, the existence of possible isomers (*) was evident, further aggravating the problem. For many species in this size range, only the ground state transition was resolved for $n \leqslant 41$. For $n>41$, no features were resolved and the PES spectra became essentially continuous. Ion mobility experiments[29,30] suggest that tin clusters gradually rearrange towards near spherical geometries in the size range of $n \sim 35-65$. Our PES spectra indicate that this structural transition may occur around Sn_{42}, since continuous spectra were suddenly observed beyond $n=42$. The featureless PES spectra may result from the metalliclike behavior of the large tin clusters, as will be discussed below.

In the larger cluster size range, the spectrum of Sn_{29}^- was somewhat special with well resolved spectral features and an unusually large energy gap. The most surprising observation was the spectrum of Sn_{40}^-, which was well resolved in sharp contrast to the nearly continuous spectra in this size range. These observations suggested that Sn_{29}^- and Sn_{40}^- were likely to have relatively stable and high-symmetry structures. The spectrum of Sn_{41}^- was also well resolved and displayed similarities to that of Sn_{40}^-, suggesting that the additional atom in Sn_{41}^- does not distort the Sn_{40}^- structure too much and providing strong evidence for the high stability of the Sn_{40}^- cluster.

E. EA and HOMO-LUMO gap as a function of size: Semiconductor-to-metal transition

The EAs obtained for Sn_n from the current work are given in Table I and compared with previously reported values. For $n=4-8$, our data are consistent with those of Moravec *et al.*,[50] but in the size range of $n=9-12$, our data are much more accurate because Moravec *et al.* were only able to give a range of values. Negishi *et al.*[51] reported EAs for a large set of Sn_n clusters, but most of their EA values were underestimated because of the poor resolution and the hot band transitions that led to low binding energy tails. Their EAs were in general between 0.2 and 0.5 eV too low. For Sn_{12}, their EA was too low by 0.88 eV. Our EAs are plotted as a function of size in Fig. 3(a). Large size variations are observed for small clusters of $n \leqslant 12$. Distinct minima are seen in the EA vs n curve at $n=4$, 7, 17, 29, 36, and 40. Interestingly, these EA minima correspond to maxima in the HOMO-LUMO gaps (Fig. 4), suggesting that the corresponding neutral clusters exhibit pronounced stability. In Fig. 3(b), we plotted the EAs as a function of $n^{-1/3}$, i.e., $1/r$, where r is the cluster radius and is proportional to $n^{1/3}$. It is seen that the EAs follow in general a straight line, which extrapolates to 4.4 eV at infinite cluster size, very close to the bulk work function of tin (4.42 eV). The EAs for clusters above $n=42$ fall on the straight line, suggesting that the large clusters can be described by the classical metallic droplet model.[58]

In Fig. 4 we plotted the HOMO-HUMO gaps of Sn_n clusters as a function of size. All clusters up to $n=41$ display a HOMO-LUMO gap, suggesting that these clusters are semiconductorlike with a closed shell electronic configuration. The HOMO-LUMO gaps are strongly dependent on the cluster size. In addition to the unusually large gaps shown by Sn_4 and Sn_7, there are other pronounced maxima at $n=16-18$, 22, 29, 36, and 40, which correspond to the EA minima, as mentioned above. The HOMO-HUMO gap disappeared precipitously for clusters with $n \geqslant 42$, suggesting that the larger clusters are metalliclike. The semiconductor-to-metal transition at $n=42$ is also accompanied by the abrupt change in the PES spectral pattern and the EA vs $1/r$ curve [Fig. 3(b)], which shows that the EAs of clusters above $n=42$ can be described by the metallic droplet model.[58]

V. CONCLUSIONS

A photoelectron spectroscopy study was carried out for Sn_n^- ($n=4-45$) clusters at two detachment photon energies, 193 and 266 nm, under well controlled experimental conditions to produce relatively cold cluster anions. Well resolved PES spectra were obtained for small clusters with $n=4-25$ and surprisingly for two large clusters, Sn_{29}^- and Sn_{40}^-. The well resolved spectra can be used to compare with future theoretical calculations to elucidate the detailed structures of the tin clusters. The PES spectra of very small Sn_n^- clusters ($n=4-13$) were compared with those of Si_n^- and Ge_n^- clusters, and both similarities and differences were observed, depending on the size. More accurate electron affinities for tin clusters were obtained and the evolution of their electronic structure was systematically investigated. A HOMO-LUMO gap was observed in the PES spectra for clusters with $n \leqslant 41$, indicating the semiconductor nature of small tin clusters. A semiconductor-to-metal transition was observed at $n=42$, beyond which no energy gaps were observed and the PES spectra became featureless and continuous.

ACKNOWLEDGMENTS

This work was supported by the National Science Foundation (DMR-0503383) and performed at the W.R. Wiley Environmental Molecular Sciences Laboratory, a national scientific user facility sponsored by the DOE's Office of Biological and Environmental Research and located at Pacific Northwest National Laboratory, operated for the DOE by Battelle.

[1] W. L. Brown, Science **235**, 860 (1987).
[2] M. F. Jarrold, Science **252**, 1085 (1991).
[3] E. C. Honea, A. Ogura, C. A. Murray, K. Raghavachari, W. O. Sprenger, M. F. Jarrold, and W. L. Brown, Nature (London) **366**, 42 (1993).
[4] Q. L. Zhang, Y. Liu, R. F. Curl, F. K. Tittel, and R. E. Smalley, J. Chem. Phys. **88**, 1670 (1988).
[5] S. Li, R. J. Van Zee, W. Weltner, Jr., and K. Raghavachari, Chem. Phys. Lett. **243**, 275 (1995).
[6] S. H. Cheshnovsky, S. H. Yang, C. L. Pettiette, M. J. Craycraft, Y. Liu, and R. E. Smalley, Chem. Phys. Lett. **138**, 119 (1987).
[7] C. C. Arnold and D. M. Neumark, J. Chem. Phys. **99**, 3353 (1993).
[8] C. Xu, T. R. Taylor, G. R. Burton, and D. M. Neumark, J. Chem. Phys. **108**, 1395 (1998).
[9] M. Maus, G. Gantefor, and W. Eberhardt, Appl. Phys. A: Mater. Sci. Process. **70**, 535 (2000).
[10] M. A. Hoffmann, G. Wrigge, B. v. Issendorff, J. Muller, G. Gantefor, and H. Haberland, Eur. Phys. J. D **16**, 9 (2001).
[11] S. Ogut, J. R. Chelikowsky, and S. G. Louie, Phys. Rev. Lett. **79**, 1770 (1997).
[12] J. Muller, B. Liu, A. A. Shvartsburg, S. Ogut, J. R. Chelikowsky, K. W.

M. Siu, K. M. Ho, and G. Gantefor, Phys. Rev. Lett. **85**, 1666 (2000).
[13] J. Bai, L. F. Cui, J. Wang, S. Yoo, X. Li, J. Jellinek, C. Koehler, T. Frauenheim, L. S. Wang, and X. C. Zeng, J. Phys. Chem. A **110**, 908 (2006).
[14] Y. Negishi, H. Kawamata, F. Hayakawa, A. Nakajima, and K. Kaya, Chem. Phys. Lett. **294**, 370 (1998).
[15] G. R. Burton, C. Xu, C. C. Arnold, and D. M. Neumark, J. Chem. Phys. **104**, 2757 (1996).
[16] M. F. Jarrold and J. E. Bower, J. Chem. Phys. **96**, 9180 (1992).
[17] K. M. Ho, A. A. Shvartsburg, B. Pan, Z. Y. Liu, C. Z. Wang, J. G. Wacker, J. L. Fye, and M. F. Jarrold, Nature (London) **392**, 582 (1998).
[18] J. M. Hunter, J. L. Fye, M. F. Jarrold, and J. E. Bower, Phys. Rev. Lett. **73**, 2063 (1994).
[19] A. A. Shvartsburg, B. Liu, Z. Y. Lu, C. Z. Wang, M. F. Jarrold, and K. M. Ho, Phys. Rev. Lett. **83**, 2167 (1999).
[20] A. A. Shvartsburg, B. Liu, M. F. Jarrold, and K. M. Ho, J. Chem. Phys. **112**, 4517 (2000).
[21] R. R. Hudgins, M. Imai, M. F. Jarrold, and P. Dugourd, J. Chem. Phys. **111**, 7865 (1999).
[22] Q. Sun, Q. Wang, P. Jena, S. Waterman, and Y. Kawazoe, Phys. Rev. A **67**, 063201 (2003).
[23] S. Yoo, X. C. Zeng, X. Zhu, and J. Bai, J. Am. Chem. Soc. **125**, 13318 (2003).
[24] S. Yoo, J. J. Zhao, J. Wang, and X. C. Zeng, J. Am. Chem. Soc. **126**, 13845 (2004).
[25] S. Yoo and X. C. Zeng, Angew. Chem., Int. Ed. **44**, 1491 (2005).
[26] S. Ogut and J. R. Chelikowsky, Phys. Rev. B **55**, R4914 (1997).
[27] J. Wang, G. Wang, and J. Zhao, Phys. Rev. B **64**, 205411 (2001).
[28] S. Bulusu, S. Yoo, and X. C. Zeng, J. Chem. Phys. **122**, 164305 (2005).
[29] A. A. Shvartsburg and M. F. Jarrold, Phys. Rev. A **60**, 1235 (1999).
[30] A. A. Shvartsburg and M. F. Jarrold, Chem. Phys. Lett. **317**, 615 (2000).
[31] A. A. Shvartsburg and M. F. Jarrold, Phys. Rev. Lett. **85**, 2530 (2000).
[32] C. Majumder, V. Kumar, H. Mizuseki, and Y. Kawazoe, Phys. Rev. B **64**, 233405 (2001).
[33] C. Majumder, V. Kumar, H. Mizuseki, and Y. Kawazoe, Phys. Rev. B **71**, 035401 (2005).
[34] K. Joshi, D. G. Kanhere, and S. A. Blundell, Phys. Rev. B **67**, 235413 (2003).
[35] S. Krishnamurty, K. Joshi, D. G. Kanhere, and S. A. Blundell, Phys. Rev. B **73**, 045419 (2006).
[36] F. C. Chuang, C. Z. Wang, S. Ogut, J. R. Chelikowsky, and K. M. Ho, Phys. Rev. B **69**, 165408 (2004).
[37] G. A. Breaux, C. M. Neal, B. Cao, and M. F. Jarrold, Phys. Rev. B **71**, 073410 (2005).
[38] L. F. Cui, X. Huang, L. M. Wang, D. Y. Zubarev, A. I. Boldyrev, J. Li, and L. S. Wang, J. Am. Chem. Soc. **128**, 8391 (2006).
[39] W. G. Burgers and L. J. Groen, Discuss. Faraday Soc. **23**, 183 (1957).
[40] K. LaiHing, R. G. Wheeler, W. L. Wilson, and M. A. Duncan, J. Chem. Phys. **87**, 3401 (1987).
[41] T. P. Martin and H. Schaber, J. Chem. Phys. **83**, 855 (1985).
[42] M. Watanabe, Y. Saito, S. Nishigaki, and T. Noda, Jpn. J. Appl. Phys., Part 1 **27**, 427 (1988).
[43] S. Yoshida and K. Kuke, J. Chem. Phys. **111**, 3880 (1999).
[44] A. B. Anderson, Chem. Phys. **63**, 4430 (1975).
[45] D. Dai and K. Balasubramanian, J. Chem. Phys. **96**, 8345 (1991).
[46] D. Dai and K. Balasubramanian, J. Phys. Chem. **100**, 19321 (1996).
[47] B. Wang, L. M. Molina, M. J. Lopez, A. Rubio, J. A. Alonso, and M. J. Scott, Ann. Phys. **7**, 107 (1998).
[48] Z.-Y. Lu, C.-Z. Wang, and K. M. Ho, Phys. Rev. B **61**, 2329 (2000).
[49] G. Gantefor, M. Gausa, K. H. Meiwes-Broer, and H. O. Lutz, Z. Phys. D: At., Mol. Clusters **12**, 405 (1989).
[50] V. D. Moravec, S. A. Klopcic, and C. C. Jarrold, J. Chem. Phys. **110**, 5079 (1999).
[51] Y. Negishi, H. Kawamata, A. Nakajima, and K. Kaya, J. Electron Spectrosc. Relat. Phenom. **106**, 117 (2000).
[52] L. F. Cui, X. Huang, L. M. Wang, J. Li, and L. S. Wang, J. Phys. Chem. A **110**, 10169 (2006).
[53] L. F. Cui, X. Huang, L. M. Wang, J. Li, and L. S. Wang, Angew. Chem., Int. Ed. **46**, 742 (2007).
[54] T. Guo, R. E. Smalley, and G. E. Scuseria, J. Chem. Phys. **99**, 352 (1993).
[55] L. S. Wang and H. Wu, in *Cluster Materials*, Advances in Metal and Semiconductor Clusters Vol. IV, edited by M. A. Duncan (JAI, Greenwich, CT, 1998, pp. 299–343.
[56] J. Akola, M. Manninen, H. Hakkinen, U. Landman, X. Li, and L. S. Wang, Phys. Rev. B **60**, R11297 (1999).
[57] L. S. Wang and X. Li, in *Clusters and Nanostructure Interfaces*, edited by P. Jena, S. N. Khanna, and B. K. Rao (World Scientific, River Edge, NJ, 2000) pp. 293–300.
[58] D. M. Wood, Phys. Rev. Lett. **46**, 749 (1981).